PERGAMON

Available online at www.sciencedirect.com

SCIENCE DIRECT®

Polyhedron 22 (2003) 1735–1743

POLYHEDRON

www.elsevier.com/locate/poly

Using HgX_2 units (X = Cl, CN) to increase structural and magnetic dimensionality in conjunction with (2,2′-bipyridyl)copper(II) building blocks

Daniel B. Leznoff *, Neil D. Draper, Raymond J. Batchelor

Department of Chemistry, Simon Fraser University, 8888 University Drive, Burnaby, BC, Canada V5A 1S6

Received 6 October 2002; accepted 10 February 2003

Abstract

A series of complexes containing $(bipy)_nCuCl_2$ units (bipy = 2,2′-bipyridyl; $n = 1,2$) and linear, neutral $Hg(CN)_2$ or $HgCl_2$ building blocks have been synthesized and structurally characterized. Generally, the Lewis acidic HgX_2 moieties accept chloride ligands from the copper(II) center, in some cases increasing the structural and magnetic dimensionality of the system as a result. $[Cu(bipy)_2(\mu\text{-}Cl)_2Hg(CN)_2]$ (**1**) is a molecular complex in which the chloride ligands bridge the copper(II) and mercury(II) centers. $[Cu(bipy)_2Hg_2Cl_6]_2$ (**2**) contains two copper(II) centers connected by an $[Hg_4Cl_{12}]^{4-}$ bridge, that was generated by chloride migration from the harder copper(II) to the softer, highly Lewis acidic $HgCl_2$ group. N-cyano coordination from $Hg(CN)_2$ in $\{[Cu(bipy)Hg(CN)_2Cl_2]_2Hg(CN)_2\}$ (**3**) generates a "Chinese-kite" type Cu_2Hg_2 rectangular cluster. The clusters are connected to form a 1D chain by $Hg(CN)_2$ groups, that accept bridging chloride ligands from adjoining clusters. The crystallization of $(bipy)CuCl_2/Hg(CN)_2$-containing complexes from aqueous NH_4OH yields 1D $\{[Cu(bipy)(OH)(Cl)]_2Hg(CN)_2\}\cdot 2H_2O$ (**4**) which is composed of $[(bipy)Cu(OH)(Cl)]_2$ units bridged by $Hg(CN)_2$ moieties. The variable temperature magnetic susceptibility of **3** can be fitted to the theoretical expression for a 1D antiferromagnetic chain of $S = 1/2$ centers with alternating interaction pathways ($J = -0.92$ cm^{-1}, $\alpha = 0.17$, $g = 2.26$). For **4**, μ_{eff} increases with decreasing temperature to a maximum and then decreases; fitting with the Bleaney–Bowers model for copper(II) dimers with weak antiferromagnetic interdimer interactions yielded $J = 56.3$ cm^{-1}, $zJ' = -0.06$ cm^{-1} and $g = 2.23$. Complexes **3** and **4** are examples of coordination polymers with the rarely used $Hg(CN)_2$ building block.

Keywords: Cu(II) complexes; Mercury; Cyanide ligands; Coordination polymers; Magnetic properties

1. Introduction

Anionic cyanometallate complexes have been extremely valuable in the study of supramolecular coordination polymers, particularly in molecular magnetism research, as they readily form polymers when reacted with transition metal cations, as well as promoting strong magnetic exchange [1]. Most research has focused on the reaction of octahedral $[M(CN)_6]^{n-}$ units with other transition metal cations [2–4], although some square-planar, hepta- and octanuclear cyanometallates have also been employed [5–8]. However, two-coordinate, linear metal cyanides have not been extensively explored as building blocks in supramolecular inorganic chemistry, despite their aforementioned general utility both as a cyanometallate and as a linear-directing building block, such as 4,4′-bipyridine, in the formation of coordination polymers [9].

With this in mind, we have targeted the use of linear, anionic $[M(CN)_2]^-$ units (M = Au [10–12], Ag [13]) as building blocks in coordination polymers. Both the silver and gold cyanometallates were shown to be capable of increasing structural dimensionality by forming metallophilic (M···M) interactions and, although diamagnetic, can propagate significant magnetic interactions [10,13]. As a comparison, we have been exploring the use of mercury(II) cyanide, $Hg(CN)_2$, a linear but neutral building block [14]. The $Hg(CN)_2$ unit is known to react with simple salts such as MX

---

* Corresponding author. Tel.: +1-604-291-4887; fax: +1-604-291-3765.

E-mail address: dleznoff@sfu.ca (D.B. Leznoff).

0277-5387/03/$ - see front matter © 2003 Elsevier Science Ltd. All rights reserved.
doi:10.1016/S0277-5387(03)00201-8

(M = Na, K, Rb, Cs; X = NCO, NCS, N_3, CN, Cl, Br, I; sometimes HgX_2 is also added) [15,16], $(R_4N)CN/M'CN$ (M′ = Li, Na, K, Cu) [17] or $M''(NCS)_2$ (M″ = Mg, Ca, Sr, Ba) [18] to yield solid-state "double-salt" arrays of the form $MHg(CN)_2X$, $R_4NM'Hg(CN)_4$ or $M''[Hg(CN)_2(SCN)]_2$, respectively. However, $Hg(CN)_2$ has only very recently been utilized as a building block to form more complex coordination polymers [14]. The coordinatively unsaturated Hg(II) center provides an interesting design possibility: not only could linear, bridging $Hg(CN)_2$ units be incorporated into coordination polymers by virtue of the cyano-N ligand binding to a transition metal, but they could also form the basis for in situ generated square-planar, tetrahedral or higher coordinate moieties by accepting compatible ligands during polymer formation [19,20]. This process could potentially increase both the structural and magnetic dimensionality in the supramolecular polymer that is generated.

We report here, the synthesis, structural and magnetic properties of a series of (2,2′-bipyridyl)copper(II) complexes that have been reacted with coordinatively unsaturated $Hg(CN)_2$ and for comparison, $HgCl_2$, to generate multinuclear and multidimensional systems. These supramolecular complexes represent some of the first examples of $Hg(CN)_2$-containing coordination polymers and illustrate that Hg(II) centers can propagate significant magnetic interactions.

2. Experimental

2.1. General procedures and physical measurements

All manipulations were performed in air using purified solvents. All reagents were obtained from commercial sources and used as received. IR spectra were obtained using a Thermo Nicolet 120 FTIR spectrometer. Microanalyses (C, H, N) were performed at Simon Fraser University by Mr. Miki Yang.

Magnetic susceptibility data were collected using a Quantum Design SQUID MPMS-5S magnetometer working down to 2 K at 1 T field strength. Samples were measured in a cylindrical, airtight sample holder constructed from PVC [21]. The data were corrected for TIP, the diamagnetism of the sample holder and the constituent atoms (by use of Pascal constants) [22].

2.2. Synthetic procedures

2.2.1. $[Cu(bipy)_2(\mu\text{-}Cl)_2Hg(CN)_2]$ (1)

To a 15 ml aqueous solution of $CuCl_2 \cdot 2H_2O$ (0.067 g, 0.39 mmol), a methanolic solution of bipy (stock solution, 0.79 mmol) was added dropwise with stirring. A 10 ml aqueous solution of $Hg(CN)_2$ (0.100 g, 0.40 mmol) was added with stirring to this solution. The mixture was allowed to slowly evaporate. Bluish-green crystal blocks of $[Cu(bipy)_2(\mu\text{-}Cl)_2Hg(CN)_2]$ (**1**) were collected by vacuum filtration, washed with cold H_2O, and were left to air dry. Yield: 0.207 g (75%). Anal. Calc. for $C_{22}H_{16}N_6Cl_2CuHg$: C, 37.78; H, 2.31; N, 12.02. Found: C, 38.05; H, 2.27; N, 12.05%. IR (KBr, cm^{-1}): ν(CN) 2172 (w), ν(CN) 2146 (w), 1605 (s), 1566 (m), 1494 (m), 1477 (s), 1443 (s), 1419 (m), 1319 (s), 1252 (m), 1221 (w), 1186 (m), 1163 (s), 1105 (w), 1063 (m), 1027 (s), 1013 (m), 958 (w), 906 (w), 891 (w), 814 (m), 775 (s), 733 (s), 658 (s), 631 (m), 439 (w), 409 (s).

2.2.2. $[Cu(bipy)_2Hg_2Cl_6]_2$ (2)

To a 10 ml aqueous solution of $CuCl_2 \cdot 2H_2O$ (0.067 g, 0.39 mmol), a methanolic solution of bipy (stock solution, 0.79 mmol) was added dropwise with stirring. A 10 ml aqueous solution of $HgCl_2$ (0.213 g, 0.78 mmol) was added to this solution resulting in an immediate white precipitate that was left to settle. The mixture was decanted, and the pale blue solution was allowed to slowly evaporate. Small blue crystal platelets of $[Cu(bipy)_2Hg_2Cl_6]_2$ (**2**) were collected by vacuum filtration, washed with cold H_2O, and were left to air dry. Yield: 0.103 g (26%). Anal. Calc. for $C_{20}H_{16}N_4Cl_6CuHg_2$: C, 24.27; H, 1.63; N, 5.66. Found: C, 24.01; H, 1.60; N, 5.50%. IR (KBr, cm^{-1}): 1974 (w), 1935 (w), 1862 (w), 1602 (s), 1567 (m), 1493 (m), 1474 (s), 1443 (s), 1419 (m), 1316 (m), 1251 (m), 1215 (w), 1172 (m), 1157 (m), 1105 (m), 1066 (m), 1044 (w), 1028 (m), 1014 (m), 973 (w), 901 (m), 810 (w), 769 (vs), 729 (s), 660 (m), 634 (w), 496 (w), 439 (w), 419 (m).

2.2.3. $\{[Cu(bipy)Hg(CN)_2Cl_2]_2Hg(CN)_2\}$ (3)

To a 15 ml aqueous solution of $CuCl_2 \cdot 2H_2O$ (0.067 g, 0.39 mmol), a methanolic solution of bipy (stock solution, 0.39 mmol) was added dropwise with stirring. A 10 ml aqueous solution of $Hg(CN)_2$ (0.150 g, 0.59 mmol) was added to this solution. The mixture was allowed to slowly evaporate. Blue crystal blocks of $\{[Cu(bipy)Hg(CN)_2Cl_2]_2Hg(CN)_2\}$ (**3**) were collected by vacuum filtration, washed with cold H_2O, and were left to air dry. Yield: 0.171 g (65%). Anal. Calc. for $C_{16}H_8N_8Cl_2CuHg_3$: C, 23.32; H, 1.20; N, 10.46. Found: C, 23.12; H, 1.21; N, 10.43%. IR (KBr, cm^{-1}): ν(CN) 2242 (m), ν(CN) 2182 (w), 1952 (w), 1874 (w), 1612 (s), 1602 (vs), 1567 (m), 1498 (s), 1474 (s), 1445 (vs), 1312 (s), 1251 (m), 1224 (w), 1173 (s), 1154 (s), 1110 (m), 1061 (m), 1033 (s), 1020 (m), 977 (m), 808 (m), 778 (vs), 748 (m), 730 (vs), 662 (m), 650 (m), 640 (m), 502 (s), 434 (m), 421 (m).

2.2.4. $\{[Cu(bipy)(OH)(Cl)]_2Hg(CN)_2\} \cdot 2H_2O$ (4)

To a 15 ml aqueous solution of $CuCl_2 \cdot 2H_2O$ (0.067 g, 0.39 mmol), a methanolic solution of bipy (stock solution, 0.39 mmol) was added dropwise with stirring. A 10 ml aqueous solution of $Hg(CN)_2$ (0.050 g, 0.20

mmol) was added to this solution. The mixture was made basic by the addition of 10 ml NH_4OH (conc.) and allowed to slowly evaporate. Dark blue plate-shaped crystals of $\{[Cu(bipy)(OH)(Cl)]_2Hg(CN)_2\}\cdot 2H_2O$ (**4**) were collected by vacuum filtration, washed with cold H_2O, and were left to air dry. Yield: 0.080 g (49%). Anal. Calc. for $C_{22}H_{22}N_6O_4Cl_2Cu_2Hg$: C, 31.72; H, 2.66; N, 10.09. Found: C, 31.61; H, 2.60; N, 9.89%. IR (KBr, cm^{-1}): ν(CN) 2182 (w), 2034 (w), 1605 (s), 1568 (w), 1500 (m), 1479 (m), 1446 (s), 1321 (m), 1255 (w), 1162 (m), 1108 (m), 1032 (m), 1018 (w), 979 (m), 949 (m), 913 (w), 770 (s), 747 (m), 732 (s), 661 (m), 638 (m), 532 (w), 482 (m), 431 (m).

2.3. *X-ray crystallographic analysis of **1–4***

Crystallographic data for all structures are collected in Table 1. All crystals were mounted on glass fibers using epoxy adhesive. The data was collected at room temperature using the diffractometer control program DIFRAC [23] and an Enraf Nonius CAD4F diffractometer. The data was corrected for the effects of absorption using a semi-empirical psi-scan method. Data reduction for all compounds included corrections for Lorentz and polarization effects.

For **1**, **3** and **4**, coordinates and anisotropic displacement parameters for the non-hydrogen atoms were refined; for compound **2** the carbon atoms were refined using isotropic thermal parameters. In **4**, H(11), H(12) and H(13) were located, and their coordinates and isotropic thermal parameters refined. All other hydrogen atoms in the structures were placed in calculated positions (d C–H 0.95 Å) and their coordinate shifts were linked with those of the respective carbon atoms during refinement. Isotropic thermal parameters for all hydrogen atoms were initially assigned proportionately to the equivalent isotropic thermal parameters of their respective carbon or oxygen atoms. Subsequently, the isotropic thermal parameters for the C–H and O–H (in **4**) hydrogen atoms were constrained to have identical shifts during refinement. An extinction parameter [24] was included in the final cycles of full-matrix least-squares refinement of **3**. Selected bond lengths and angles for **1**, **2**, **3**, and **4** are found in Tables 2–5, respectively.

The programs used for all absorption corrections, data reduction and processing of **1–4** were from the NRCVAX crystal structure system [25]. The structure was solved and refined using CRYSTALS [26]. Complex scattering factors for neutral atoms [27] were used in the calculation of structure factors.

3. Results and discussion

3.1. *Synthesis and characterization of Cu(II)–Hg(II) complexes*

The reaction of an aqueous/methanolic solution of $CuCl_2$ containing 1 or 2 equiv. of 2,2′-bipyridine (bipy) with an aqueous solution of HgX_2 (X = CN, Cl) yielded single crystals of products **1–4** after partial evaporation

Table 1
Summary of crystallographic data

	1	**2**	**3**	**4**
Empirical formula	$C_{22}H_{16}N_6Cl_2CuHg$	$C_{20}H_{16}N_4Cl_6CuHg_2$	$C_{13}H_8N_5Cl_2CuHg_{1.5}$	$C_{11}H_{11}N_3O_2ClCuHg_{0.5}$
Formula weight ($g\ mol^{-1}$)	699.45	989.82	669.58	416.52
Crystal system	triclinic	triclinic	triclinic	triclinic
Space group	$P\bar{1}$	$P\bar{1}$	$P\bar{1}$	$P\bar{1}$
a (Å)	8.963(4)	9.754(2)	7.913(3)	7.185(2)
b (Å)	12.107(4)	11.557(2)	8.384(1)	9.460(2)
c (Å)	12.141(7)	12.504(3)	13.584(3)	10.627(2)
α (°)	83.30(5)	82.02(2)	81.35(2)	106.35(2)
β (°)	69.60(4)	70.91(2)	73.33(3)	96.51(2)
γ (°)	68.19(3)	85.56(2)	75.60(2)	109.28(2)
Z	2	2	2	2
V (Å^3)	1146.34	1318.35	833.16	637.04
D_{calc} ($g\ cm^{-3}$)	2.026	2.494	2.669	2.171
2θ Range (°)	4–50	4–45	4–58	4–52
Reflections collected	5812	4077	4987	3115
Independent reflections	4070	3469	4465	2512
Reflections observed [$I = 2.5\sigma(I)$]	3204	1683	3164	2039
GoF[a]	0.819	1.141	1.923	1.147
R_F, R_{wF} [$I_O \geq 2.5\sigma(I)$][a]	0.029, 0.0284	0.042, 0.0454	0.0294, 0.035	0.021, 0.0224

[a] $R_F = \Sigma|(|F_O| - |F_C|)/\Sigma|F_O|$, for observed data ($I_O \geq 2.50(I)$).
$R_W F = [\Sigma(w(|F_O| - |F_C|)^2)/\Sigma(wF_O^2)]^{1/2}$ for observed data.
$GoF = [\Sigma(w(F_O - F_C|)^2)/\text{degrees of freedom}]^{1/2}$.

of the resulting solutions. In each case, preferential binding or even complete migration of the labile chloride ligands from the harder Cu(II) center to the coordinatively unsaturated, softer Hg(II) center drives the formation of the products [19,20]. As a result, products **1**–**4** all contain non-linear Hg(II) units with a coordination number greater than two, potentially increasing the structural dimensionality in the process.

The IR spectra of **1**, **3** and **4** clearly show the presence of the CN groups, and also reflect their chemical environment. The ν_{CN} bands from 2146 to 2182 cm^{-1} are consistent with terminal cyanide groups on four-coordinate mercury(II) centers, such as in $[Hg(CN)_2Cl_2]^{2-}$ anions [28]. In **3**, the band at 2242 cm^{-1} is assigned to the cyanide moiety that bridges directly to the Cu(II) metal center; this large shift to higher energy is generally identified with N-bridging cyanides [1]. All bands are shifted from the 2194 cm^{-1} absorbance of unligated $Hg(CN)_2$ [29]. The solid-state structures of all the complexes are described below.

*3.2. Structures and magnetic properties of [Cu(bipy)$_2$(μ-Cl)$_2$Hg(CN)$_2$] (**1**) and [Cu(bipy)$_2$Hg$_2$Cl$_6$]$_2$ (**2**)*

Single crystals of **1** and **2** were obtained by slow evaporation of solutions containing $(bipy)_2CuCl_2$ and 1 equiv. of $Hg(CN)_2$ or 2 equiv. of $HgCl_2$, respectively. The X-ray crystal structure of [Cu(bipy)$_2$(μ-Cl)$_2$Hg(CN)$_2$] (**1**) reveals a simple molecular complex, in which the coordinatively unsaturated $Hg(CN)_2$ unit is bound to the chloride ligands, which act as Cu–Hg bridging groups (Fig. 1). The Cu(II) center in **1** has an axially distorted, octahedral geometry, with two 2,2′-bipyridine ligands *cis*-oriented and two chloride atoms completing the coordination sphere. The Cu(1)–N bond lengths range from 1.996(3) and 2.087(4) Å in the equatorial plane to 2.189(4) Å in the Jahn–Teller distorted axial site (Table 2). The equatorial and axial Cu(1)–Cl bond lengths are 2.443(1) and 2.786(1) Å, respectively, which can be compared with the 2.218(19) and 2.723(38) Å found in the equatorial/axial Cu–Cl bonds [30] in the chloride-bridged $[(terpy)CuCl]_2[PF_6]_2$ or the 2.481(1) and 2.545(2) Å found in the distorted, chloride-bridged $[(dpt)CuCl]_2(Cl)_2$ (dpt = dipropylenetriamine) [31]. The chloride ligands bridge to the $Hg(CN)_2$ metal center via Hg(1)–Cl bonds of 2.820(1) and 2.710(1) Å, yielding a distorted see-saw geometry around the Hg(1) center (C(11)–Hg(1)–C(12) = 160.6(2)°). The Cu–Hg distance is 3.918 Å, but there are no significant intermolecular interactions. In short, the addition of $Hg(CN)_2$ to coordinatively saturated $(bipy)_2CuCl_2$ does not induce halide migration and no coordination sites are opened on the Cu(II) center: no increase in structural or magnetic dimensionality is observed.

Table 2
Selected bond lengths (Å) and angles (°) for [Cu(bipy)$_2$(μ-Cl)$_2$Hg(CN)$_2$] (**1**)

Bond lengths			
Cu(1)–N(1)	1.999(3)	Cu(1)–N(2)	2.189(4)
Cu(1)–N(3)	1.996(3)	Cu(1)–N(4)	2.087(4)
Cu(1)–Cl(1)	2.443(1)	Cu(1)–Cl(2)	2.786(1)
Hg(1)–C1(1)	2.820(1)	Hg(1)–Cl(2)	2.710(1)
Hg(1)–C(12)	2.059(5)	Hg(1)–C(12)	2.051(5)
Bond angles			
N(1)–Cu(1)–N(2)	78.64(14)	N(1)–Cu(1)–N(3)	173.28(17)
N(1)–Cu(1)–N(4)	95.05(14)	N(2)–Cu(1)–N(3)	96.79(14)
N(2)–Cu(1)–N(4)	93.77(14)	N(3)–Cu(1)–N(4)	80.24(14)
N(1)–Cu(1)–Cl(1)	89.03(11)	N(1)–Cu(1)–Cl(2)	96.23(11)
N(2)–Cu(1)–Cl(1)	92.10(10)	N(2)–Cu(1)–Cl(2)	174.60(10)
N(3)–Cu(1)–Cl(1)	96.11(12)	N(3)–Cu(1)–Cl(2)	88.20(10)
N(4)–Cu(1)–Cl(1)	173.40(10)	N(4)–Cu(1)–Cl(2)	84.90(10)
Cu(1)–Cl(1)–Hg(1)	95.86(4)	Cu(1)–Cl(2)–Hg(1)	90.86(4)
Cl(1)–Hg(1)–C(11)	93.94(16)	Cl(1)–Hg(1)–C(12)	98.30(16)
Cl(2)–Hg(1)–C(11)	100.39(17)	Cl(2)–Hg(1)–C(12)	95.82(16)
Cl(1)–Cu(1)–Cl(2)	89.54(4)	Cl(1)–Hg(1)–Cl(2)	83.71(4)
C(11)–Hg(1)–C(12)	160.6(2)		

Similarly, the structure of [Cu(bipy)$_2$Hg$_2$Cl$_6$]$_2$ (**2**) is essentially molecular (Fig. 2). However, the copper(II) center in **2** is only five-coordinate, with a distorted geometry as exemplified by its tau parameter of $\tau = 0.47$ (where the τ range from 0 to 1 represents the geometric distortions from a perfect square-pyramid to a trigonal bipyramid, respectively) [32]. The Cu(1)–Cl(4) distance of 3.856 Å indicates that this chloride does not bind to the open Cu(II) coordination site. One chloride ligand has migrated to generate an $[HgCl_3]^-$ anion, while the remaining chloride ligand (Cu(1)–Cl(3) = 2.320(7) Å) bridges to another mercury center, resulting in the formation of a $[Hg_2Cl_6]^{2-}$ unit. The molecule dimerizes

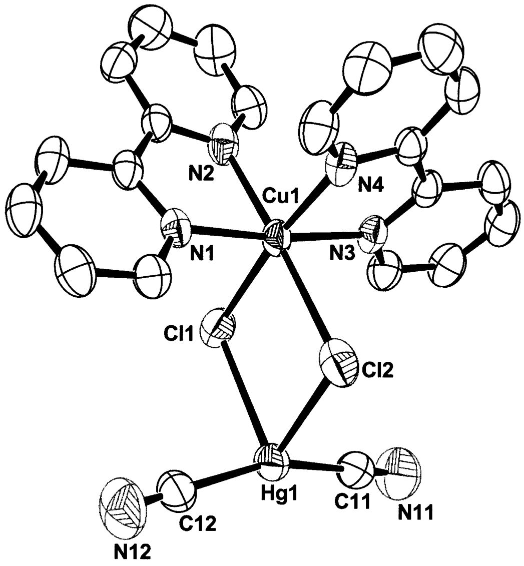

Fig. 1. Molecular structure of [Cu(bipy)$_2$(μ-Cl)$_2$Hg(CN)$_2$] (**1**) (ORTEP, 33% ellipsoids).

Table 3
Selected bond lengths (Å) and angles (°) for $[Cu(bipy)_2Hg_2Cl_6]_2$ (**2**)

Bond lengths			
Cu(1)–N(1)	1.978(17)	Cu(1)–N(2)	2.125(17)
Cu(1)–N(3)	1.973(16)	Cu(1)–N(4)	2.042(16)
Cu(1)–Cl(3)	2.320(7)	Hg(2)–Cl(3)	2.728(6)
Hg(2)–C1(4)	2.338(8)	Hg(2)–Cl(1)	2.337(7)
Hg(2)–Cl(2)	2.884(6)	Hg(1)–Cl(1)	3.112(7)
Hg(1)–Cl(2)	2.541(6)	Hg(1)–Cl(5)	2.359(6)
Hg(1)–Cl(6)	2.361(6)	Hg(1)–Cl(5*)	3.029(7)
Bond angles			
N(1)–Cu(1)–N(2)	77.8(7)	N(1)–Cu(1)–N(3)	172.0(8)
N(1)–Cu(1)–N(4)	92.3(7)	N(2)–Cu(1)–N(3)	100.9(7)
N(2)–Cu(1)–N(4)	109.0(7)	N(3)–Cu(1)–N(4)	80.6(7)
N(1)–Cu(1)–Cl(3)	93.7(6)	N(2)–Cu(1)–Cl(3)	107.0(5)
N(3)–Cu(1)–Cl(3)	94.2(5)	N(4)–Cu(1)–Cl(3)	144.0(5)
Cu(1)–Cl(3)–Hg(2)	107.3 (2)	Cl(3)–Hg(2)–Cl(1)	93.2(2)
Cl(3)–Hg(2)–Cl(2)	97.39(19)	Cl(3)–Hg(2)–Cl(4)	100.5(3)
Cl(1)–Hg(2)–Cl(2)	87.78(19)	Cl(1)–Hg(2)–Cl(4)	162.6(3)
Cl(4)–Hg(2)–Cl(2)	100.9(2)	Cl(1)–Hg(1)–Cl(2)	79.49(18)
Cl(1)–Hg(1)–Cl(5)	92.6(2)	Cl(1)–Hg(1)–Cl(6)	89.5(2)
Cl(1)–Hg(1)–Cl(5*)	170.24(19)	Cl(2)–Hg(1)–Cl(5)	110.5(2)
Cl(2)–Hg(1)–Cl(5*)	93.8(2)	Cl(2)–Hg(1)–Cl(6)	107.8(2)
Cl(5)–Hg(1)–Cl(5*)	83.1(2)	Cl(5)–Hg(1)–Cl(6)	141.4(3)
Hg(1)–Cl(5)–Hg(1*)	96.9(2)	Cl(5*)–Hg(1)–Cl(6)	99.4(2)
Hg(1)–Cl(2)–Hg(2)	96.72(19)		

Symmetry transformations: $*-x+1,\ -y+1,\ -z+1$.

via Hg–Cl bridges to yield the final structure: a dinuclear copper(II) complex with an impressive $[Hg_4Cl_{12}]^{4-}$ ribbon-like bridge. The Hg–Cl bond lengths in the bridge range from 2.337(7) to 3.112(7) Å (Table 3) and can be compared with the Hg–Cl bond lengths of 2.35, 2.40, 2.81 and 3.27 Å in $NaHgCl_3$, which is composed of twofold polymeric ribbons of $[Hg_2Cl_6]^{2-}$ units in the solid-state structure [33]. These values are all well within the sum of the Hg/Cl van der Waals radii of 3.30 Å [34]. Mercury halide anions are known to form a variety of multidimensional arrays via bridging chlorides [34–36]. This is partly a reflection of the substantially higher Lewis acidity of $HgCl_2$ compared with $Hg(CN)_2$ [37], that may also account for the increased halide migration in **2** vs. cyanide-containing **1**. The Cu(1)–Hg(2) and Hg(1)–Hg(2) distances are 4.073 and 4.059 Å, respectively; again, there are no significant intermolecular interactions.

At 300 K, $[Cu(bipy)_2(\mu\text{-}Cl)_2Hg(CN)_2]$ (**1**) has a magnetic moment $\mu_{eff} = 1.9$ BM, consistent with one $S = 1/2$ copper(II) d^9 center; no magnetic interactions are expected in this magnetically dilute complex [22]. In $[Cu(bipy)_2Hg_2Cl_6]_2$ (**2**), the Cu(1)–Cu(1*) distance of 15.4 Å precludes any significant magnetic interactions between the two d^9 centers. However, the magnetic susceptibility as a function of temperature was measured from 2 to 300 K and although Curie–Law behaviour was observed as the temperature was lowered from 300 to 15 K ($\mu_{eff} = 1.87$ BM), a small but discernable drop in magnetic moment to $\mu_{eff} = 1.81$ BM at 2 K was also noted. This apparent weak antiferromagnetic interaction may be mediated by the highly polarizable and covalent $[Hg_4Cl_{12}]^{4-}$ bridge, but the possibility that a small structural change at low temperature could activate a shorter pathway (e.g. an Hg–Cl bridge between molecular units) cannot be excluded. In any

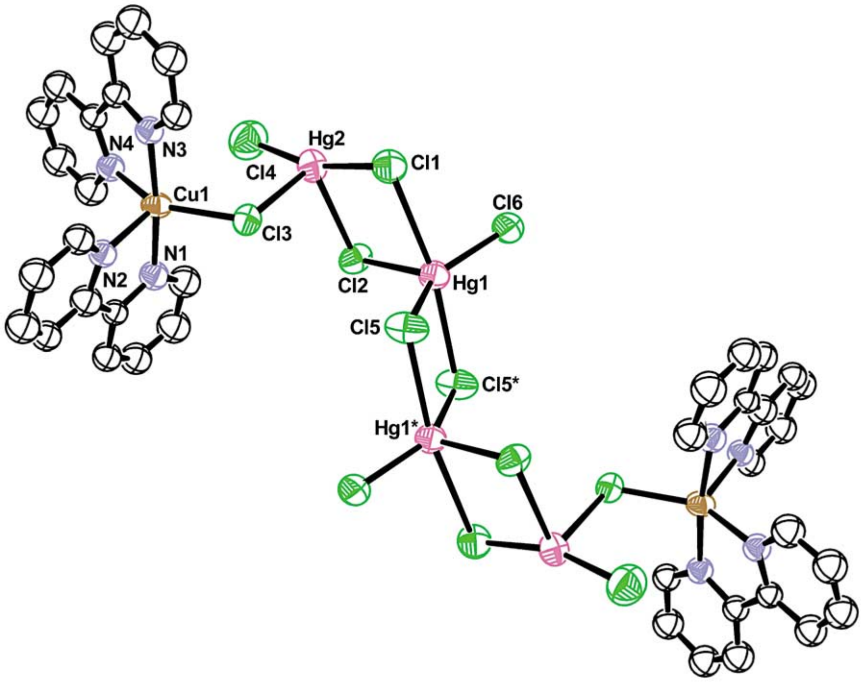

Fig. 2. Molecular structure of $[Cu(bipy)_2Hg_2Cl_6]_2$ (**2**) (ORTEP, 33% ellipsoids).

Table 4
Selected bond lengths (Å) and angles (°) for $\{[\mathrm{Cu(bipy)Hg(CN)_2Cl_2}]_2\mathrm{Hg(CN)_2}\}$ (**3**)

Bond lengths			
Cu(1)–N(1)	1.994(5)	Cu(1)–N(2)	1.998(5)
Cu(1)–Cl(1)	2.5560(17)	Cu(1)–Cl(2)	2.3090(16)
Cu(1)–N(12*)	1.967(5)	Hg(2)–Cl(1)	3.1450(16)
Hg(1)–Cl(1)	2.7867(16)	Hg(1)–Cl(2)	2.9523(16)
Hg(1)–C(11)	2.043(6)	Hg(1)–C(12)	2.042(7)
C(11)–N(11)	1.100(8)	C(12)–N(12)	1.122(8)
Hg(2)–C(21)	2.005(7)	C(21)–N(21)	1.140(9)
Bond angles			
N(1)–Cu(1)–N(2)	80.6(2)	N(1)–Cu(1)–N(12*)	165.2(2)
N(1)–Cu(1)–Cl(1)	96.95(13)	N(1)–Cu(1)–Cl(2)	94.73(14)
N(2)–Cu(1)–Cl(1)	96.27(14)	N(2)–Cu(1)–Cl(2)	164.61(15)
N(2)–Cu(1)–N(12*)	92.1(2)	Cl(1)–Cu(1)–Cl(2)	98.87(6)
Cl(1)–Cu(1)–N(12*)	96.80(18)	Cl(1)–Hg(1)–Cl(2)	80.21(4)
Cl(2)–Cu(1)–N(12*)	88.94(16)	Cl(1)–Hg(1)–C(11)	96.93(19)
Cl(1)–Hg(1)–C(12)	93.68(18)	Cl(2)–Hg(1)–C(11)	98.79(19)
Cl(2)–Hg(1)–C(12)	89.5(2)	C(11)–Hg(1)–C(12)	167.5(3)
C(12)–N(12)–Cu(1*)	177.3(6)	C(21)–Hg(2)–C(21*)	180
Cl(1)–Hg(2)–C(21)	94.6(2)	Cl(1)–Hg(2)–C(21*)	85.4(2)
Hg(1)–Cl(1)–Cu(1)	89.93(5)	Hg(1)–Cl(2)–Cu(1)	90.98(5)

Symmetry transformation: $* -x, -y+1, -z+2$.

event, the magnitude of this coupling is very small and hence was not analyzed further.

3.3. Structure and magnetic properties of $\{[Cu(bipy)Hg(CN)_2Cl_2]_2Hg(CN)_2\}$ (3)

The slow evaporation of a solution containing $\mathrm{Hg(CN)_2}$ and only 1 equiv. of bipy per $\mathrm{CuCl_2}$ moiety yielded single crystals of $\{[\mathrm{Cu(bipy)Hg(CN)_2Cl_2}]_2\mathrm{Hg(CN)_2}\}$ (**3**), the structure of which is depicted in Fig. 3. Some general structural features of **1** are present in **3** as well—the chloride ligands have not migrated from the copper(II) center, but bridge to a $\mathrm{Hg(CN)_2}$ unit via Hg(1)–Cl bonds of 2.7867(16) and 2.923(16) Å to yield a $[\mathrm{(bipy)Cu(\mu\text{-}Cl)(Cl)Hg(CN)_2}]$ moiety. The copper(II) center has a five-coordinate, square-pyramidal geometry, with one bipy, one chloride (Cu(1)–Cl(2) = 2.3090(16) Å) and one cyano-nitrogen from the adjacent $[\mathrm{(bipy)Cu(\mu\text{-}Cl)_2Hg(CN)_2}]$ group in the basal plane and the other chloride (Cu(1)–Cl(2) = 2.5560(17) Å) in the apical position completing the coordination sphere (Table 4). The Cu(1)–N(cyanide) bond length of 1.967(5) Å is typical of an equatorially bound N-cyanide to copper(II); this interaction is clearly visible as a bridging stretch in the IR spectrum of **3** (see above). The $\mathrm{Hg(CN)_2}$ units thus act as bridging ligands via the Hg(II) center to the chlorides of one copper, and via one cyano group to another copper. This unusual binding motif generates a "Chinese-kite"-shaped $\mathrm{Cu_2Hg_2}$ unit (Fig. 3) with C_i symmetry. Each tetranuclear cluster is bridged to the next one via two copper-bound chloride ligands at opposite ends of the cluster, which donate not only to Hg(1) but also to another equivalent of $\mathrm{Hg(CN)_2}$ situated between the clusters; each of these Hg(2) centers is rendered pseudo square-planar as a result. This Hg(2)–Cl(1) interaction of 3.1450(16) Å generates a 1D chain of $\mathrm{Cu_2Hg_2}$ clusters; a similar example has been reported where $\mathrm{HgCl_2}$ bridges $\mathrm{Cu_4}$ clusters [19]. Thus, the use of coordinatively unsaturated $\mathrm{Hg(CN)_2}$, which accepts chloride ligands, increases the structural dimensionality from 0 to 1 in complex **3** and is also instrumental in constructing the clusters described.

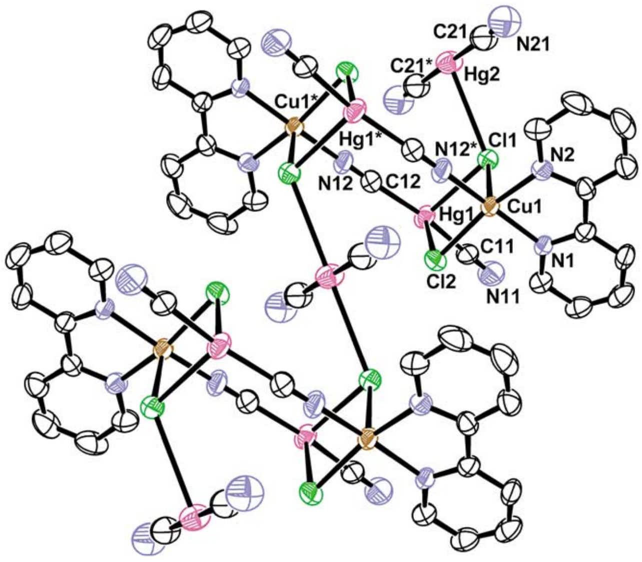

Fig. 3. Extended 1D chain structure of $\{[\mathrm{Cu(bipy)Hg(CN)_2Cl_2}]_2\mathrm{Hg(CN)_2}\}$ (**3**) (ORTEP, 33% ellipsoids).

The temperature (T) dependence of the molar magnetic susceptibility (χ_M) of a polycrystalline sample of **3** was measured in the temperature range 2–300 K. The plot of μ_{eff} vs. T is shown in Fig. 4. At 300 K, $\mu_{\mathrm{eff}} = 1.95$ BM, consistent with isolated $S = 1/2$ copper(II) centers. The μ_{eff} value remains constant until 25 K, at which point it begins to decrease, reaching a value of $\mu_{\mathrm{eff}} = 1.49$ BM at 2 K. This behaviour is consistent with the presence of weak antiferromagnetic interactions.

Examining the X-ray structure from the point of view of magnetic exchange, the Cu(1)–Cu(1*) distance within one cluster is 6.282 Å. The two through-bond magnetic pathways delineated by Cu–Cl–Hg–CN–Cu, in which the copper centers are connected in an equatorial/equatorial fashion, can mediate significant magnetic interactions [38]. In addition, copper centers on adjacent clusters are connected by axial Cl–Hg–Cl linkages, with a Cu(1)–Cu(1*) distance of 10 Å. This intercluster pathway is expected to yield weaker exchange interactions due to the longer Cu–Cu distance and axial/axial linkage. With this structural analysis in mind, the magnetic data were fitted with two different models. Firstly, using the simple Bleaney–Bowers dimer model, with $\mathscr{H} = -2 \cdot S_1 S_2$ (assuming no intercluster interactions) [22,39], the best-fit values of $J = -0.99 \pm 0.02$ cm^{-1} and $g = 2.26 \pm 0.003$ are obtained. If the second

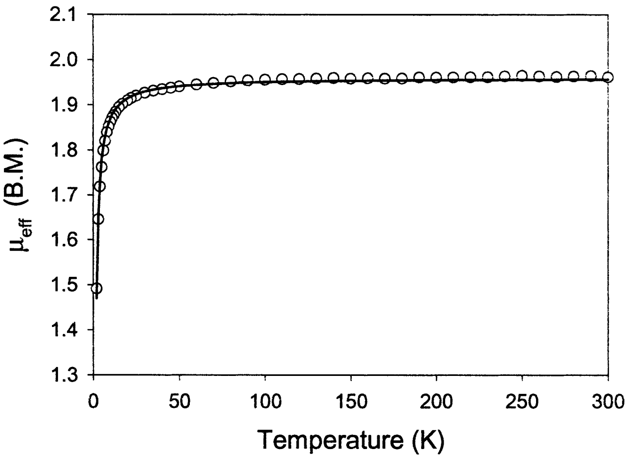

Fig. 4. Temperature dependence of μ_{eff} for **3**. The solid line is theory (see text).

pathway is included the system can in principle be treated as a 1D chain. Thus, using the theoretical expression for an alternating 1D chain of antiferromagnetically coupled $S = 1/2$ Heisenberg spins [40], the best-fit values of $J_1 = -0.92 \pm 0.01$ cm^{-1}, $\alpha = 0.17 \pm 0.01$ (i.e., the second coupling constant is αJ_1, or -0.16 cm^{-1}) and $g = 2.26 \pm 0.002$ are obtained; this fit is indicated as a solid line in Fig. 4. Even though they are weak, both pathways represent unusual examples of mercury(II) (a diamagnetic d^{10} metal center) mediating a magnetic interaction. Other d^{10} metal centers, including copper(I), gold(I), silver(I), and zinc(II) have been shown by us and others to be capable of mediating magnetic exchange [10,13,41,42].

Table 5
Selected bond lengths (Å) and angles (°) for $\{[\mathrm{Cu(bipy)(OH)(Cl)}]_2\mathrm{Hg(CN)_2}\}\cdot 2H_2O$ (**4**)

Bond lengths			
Cu(1)–N(1)	2.008(3)	Cu(1)–N(2)	2.008(3)
Cu(1)–O(2)	1.943(3)	Cu(1)–O(2*)	1.952(3)
Cu(1)–Cl(2*)	2.6709(11)	Hg(1)–C(11)	2.081(4)
C(11)–N(11)	1.077(5)	Hg(1)–Cl(2)	2.980(1)
Bond angles			
N(1)–Cu(1)–N(2)	80.82(13)	N(1)–Cu(1)–O(2*)	97.08(12)
N(1)–Cu(1)–O(2)	175.36(13)	N(2)–Cu(1)–O(2*)	159.51(14)
N(2)–Cu(1)–O(2)	97.94(13)	N(1)–Cu(1)–Cl(2*)	87.6(1)
N(2)–Cu(1)–Cl(2*)	100.1(1)	Cl(2*)–Cu(1)–O(2)	97.03(9)
Cl(2*)–Cu(1)–O(2*)	100.19(9)	C(11)–Hg(1)–C(11*)	180
O(2)–Cu(1)–O(2*)	82.51(12)	Cu(1*)–Cl(2)–Hg(1)	86.46(3)
N(11)–C(11)–Hg(1)	176.9(4)	Cl(2)–Hg(1)–C(11)	86.93(11)
Cl(2)–Hg(1)–C(11)	93.07(11)	Cu(1)–O(2)–Cu(1*)	97.49(12)

Symmetry transformations: (l(2*), Cu(1*)$-x+1$, $-y_s-z+2$; C(11*)$-x_s$, $-$y, $-z+2$.

3.4. Structure and magnetic properties of $\{[Cu(bipy)(OH)(Cl)]_2Hg(CN)_2\}\cdot 2H_2O$ (4)

If solutions containing (bipy)CuCl$_2$ and Hg(CN)$_2$ are made basic via addition of NH$_4$OH prior to solvent evaporation [43], single crystals of $\{[\mathrm{Cu(bipy)(OH)}$-$\mathrm{(Cl)}]_2\mathrm{Hg(CN)_2}\}\cdot 2H_2O$ (**4**) are obtained. The X-ray structure, shown in Fig. 5, indicates that dinuclear [(bipy)Cu(μ-OH)]$_2$ units are produced in which each copper center is square-pyramidal, with a chloride ligand in the apical position (Cu(1)–Cl(2) = 2.6709(11) Å). Within the dimer, the Cu–N, Cu–O and Cu–Cu* distances are all comparable with those found in other [(bipy)Cu(μ-OH)] systems [44].

Each dinuclear unit in **4** is connected to the next via the apical chloride ligands, which bridge to an Hg(CN)$_2$ molecule; each Hg(1) thus becomes square-planar, with Hg(1)–Cl(2) bonds of 2.980(1) Å (Table 5). This motif is similar to that observed in **3**; the chloride ligands bridge via the coordinatively unsaturated Hg(CN)$_2$ acceptors to yield a 1D chain of alternating [(bipy)Cu(μ-OH)(Cl)]$_2$ and Hg(CN)$_2$ units (Fig. 5). Thus, the Hg(CN)$_2$ units have effectively increased the structural dimensionality from 0 to 1. These chains are connected by H$_2$O molecules which form hydrogen bonds with the chlorides of one chain and N-cyano atom on the other (not

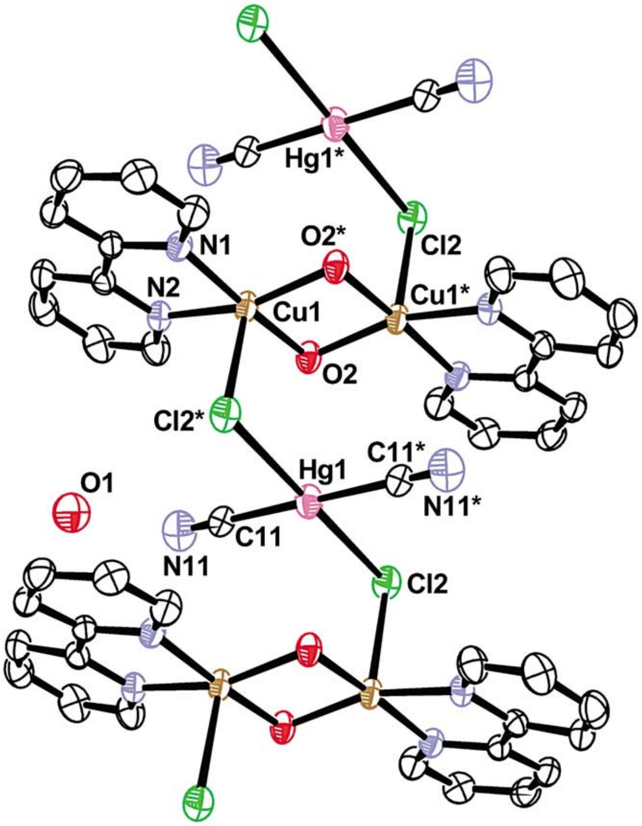

Fig. 5. Extended 1D chain structure of $\{[\mathrm{Cu(bipy)(OH)(Cl)}]_2$-$\mathrm{Hg(CN)_2}\}\cdot 2H_2O$ (**4**) (ORTEP, 33% ellipsoids).

shown) but this interaction is not magnetically significant as the distance between copper(II) centers is > 10 Å. Other coordination polymers that utilize copper(II) dimers as "complex ligands" have been reported [45,46].

Copper(II) hydroxo-bridged dimers have been extensively studied both experimentally and theoretically; the Cu–O–Cu angle and the out-of-plane O–H/R angle are known to be key geometric features that control the sign and magnitude of the coupling between $S = 1/2$ Cu(II) centers [47–49]. Specifically, Cu–O–Cu angles $> 97.5°$ generally yield antiferromagnetic coupling, while angles $< 97.5°$ generate ferromagnetic interactions [50]. The [(bipy)Cu(μ-OH)]-containing structures that have been previously reported all exhibit strongly ferromagnetic intradimer interactions, in keeping with their Cu–O–Cu angles, which range from 94.5 to 97.3° [51]; this angle is anion-dependent [44]. The critical Cu–O–Cu angle in **4** is 97.5, which is larger than that found in other [(bipy)Cu(μ-OH)] systems—on this basis alone, a small J-coupling should be observed. However, the angle of the O–H group (O–H hydrogens were located and refined in **4**) relative to the Cu_2O_2 plane is 56°, which is predicted to lead to significant ferromagnetic interactions [47,48]. To explore this point, the temperature (T) dependence of the molar magnetic susceptibility (χ_M) of a polycrystalline sample of **4** was measured and the results are depicted as a μ_{eff} vs. T plot in Fig. 6. As the temperature is lowered, μ_{eff} increases slowly from 2.04 BM at 300 K to 2.22 BM at 25 K, consistent with the presence of ferromagnetic interactions. Below 25 K, μ_{eff} decreases to a value of 2.08 BM at 2 K. The data were fitted assuming an intradimer ferromagnetic interaction and a much weaker interdimer antiferromagnetic interaction mediated through the Cl–Hg–Cl bonds; a similar intercluster pathway was identified in **3**. The data could be successfully fitted using the Bleaney–Bowers equation (as previously defined) and an additional molecular field parameter [22] with values of $J = 56.3 \pm 0.8$ cm^{-1}, $g = 2.23 \pm 0.002$ and $zJ' = -0.06 \pm 0.0004$ cm^{-1}. This result illustrates the importance of the O–H/R angle relative to the Cu_2O_2 plane in determining the sign and magnitude of the Cu–Cu coupling, as has been stressed recently [47,48]. The data could not be fitted with the 1D chain model for alternating ferromagnetic/antiferromagnetically coupled $S = 1/2$ centers [45,52] due to the relative weakness of J_{AF} vs. J_F. The slightly larger interdimer coupling constant in **3** compared with **4** can be attributed both to the shorter Cu–Cl distances (2.5560(17) Å vs. 2.6709(11) Å) and larger Cu–Cl–Hg angle (122.05(3)° vs. 86.46(3)°) in **3** vs. **4**, both of which enhance the orbital overlap necessary for magnetic exchange.

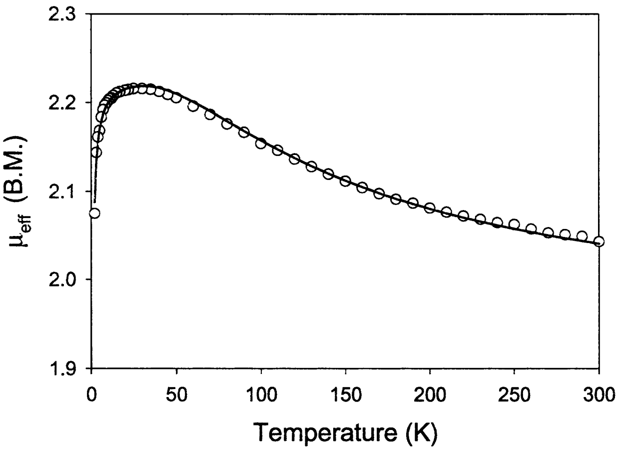

Fig. 6. Temperature dependence of μ_{eff} for **4**. The solid line is theory (see text).

4. Conclusions

Coordination polymers that incorporate linear, neutral $Hg(CN)_2$ units as ligands have been prepared, as well as a related complex using $HgCl_2$. These d^{10} centers do not form metallophilic bonds like their gold/silver counterparts [10–13,53], but can still increase structural dimensionality by acting as low-coordinate Lewis acids accepting, for example, halide ligands from complex cations in a bridging fashion. The higher Lewis acidity of $HgCl_2$ plays a role in the larger increase in structural dimensionality associated with its incorporation, compared with $Hg(CN)_2$. The mercury cyanide units mediate magnetic exchange through the diamagnetic mercury(II) center, thereby increasing the magnetic dimensionality of the coordination polymers as well. The use of these units, particularly the highly Lewis acidic $HgCl_2$, as dimensionality-enhancing building blocks in coordination polymers is under further investigation.

5. Supplementary material

Crystallographic data for the structural analysis have been deposited with the Cambridge Crystallographic Data Centre, CCDC Nos. 194864–194867 for compounds **1**–**4**, respectively. Copies of this information may be obtained free of charge from The Director, CCDC, 12 Union Road, Cambridge CB2 1EZ, UK (fax: +44-1223-336033; e-mail: deposit@ccdc.cam.ac.uk or www: http://www.ccdc.cam.ac.uk).

Acknowledgements

Financial support from Imperial Oil and NSERC of Canada is gratefully acknowledged.

References

[1] K.R. Dunbar, R.A. Heintz, Prog. Inorg. Chem. 45 (1997) 283.

[2] M. Verdaguer, A. Bleuzen, V. Marvaud, J. Vaissermann, M. Seuleiman, C. Desplanches, A. Scuiller, C. Train, R. Garde, G. Gelly, C. Lomenech, I. Rosenman, P. Veillet, C. Cartier, F. Villain, Coord. Chem. Rev. 190–192 (1999) 1023.

[3] M. Ohba, H. Okawa, Coord. Chem. Rev. 198 (2000) 313.

[4] J.S. Miller, Inorg. Chem. 39 (2000) 4392.

[5] O. Kahn, J. Larionova, L. Ouahab, Chem. Commun. (1999) 945.

[6] M. Pilkington, M. Gross, P. Franz, M. Biner, S. Decurtins, H. Stoeckli-Evans, A. Neels, J. Solid State Chem. 159 (2001) 262.

[7] D.-F. Li, S. Gao, L.-M. Zheng, K.-B. Yu, W.-X. Tang, New J. Chem. 26 (2002) 1190.

[8] T. Iwamoto, in: J.M. Lehn, J.L. Atwood, J.E.D. Davies, D.D. MacNicol, F. Vögtle, G. Alberti, T. Bein (Eds.), Comprehensive Supramolecular Chemistry, Pergamon Press, Oxford, 1996, p. 643.

[9] P.J. Hagrman, D. Hagrman, J. Zubieta, Angew. Chem., Int. Ed. Engl. 38 (1999) 2638.

[10] D.B. Leznoff, B.-Y. Xue, B.O. Patrick, V. Sanchez, R.C. Thompson, Chem. Commun. (2001) 259.

[11] D.B. Leznoff, B.-Y. Xue, C.L. Stevens, A. Storr, R.C. Thompson, B.O. Patrick, Polyhedron 20 (2001) 1247.

[12] D.B. Leznoff, B.-Y. Xue, R.J. Batchelor, F.W.B. Einstein, B.O. Patrick, Inorg. Chem. 40 (2001) 6026.

[13] C.J. Shorrock, B.-Y. Xue, P.B. Kim, R.J. Batchelor, B.O. Patrick, D.B. Leznoff, Inorg. Chem. 41 (2002) 6743.

[14] N.D. Draper, R.J. Batchelor, B.C. Sih, Z.-G. Ye, D.B. Leznoff, Chem. Mater. 15 (2003) 1612.

[15] G. Thiele, P. Hilfrich, Z. Anorg. Allg. Chem. 461 (1980) 109.

[16] G. Thiele, K. Brodersen, H. Frohring, Z. Naturforsch., Teil. B 36 (1981) 180.

[17] G. Thiele, J. Grobmann, A.W. Pürzer, Z. Naturforsch., Teil. B 41 (1986) 1346.

[18] K. Brodersen, H.U. Hummel, Z. Anorg. Allg. Chem. 500 (1983) 171.

[19] S. Wang, S.J. Trepanier, J.-C. Zheng, Z. Pang, M.J. Wagner, Inorg. Chem. 31 (1992) 2118.

[20] G. Exarchos, S.D. Robinson, J.W. Steed, Polyhedron 20 (2001) 2951.

[21] M.K. Ehlert, S.J. Rettig, A. Storr, R.C. Thompson, J. Trotter, Can. J. Chem. 67 (1989) 1970.

[22] O. Kahn, Molecular Magnetism, VCH, Weinheim, 1993.

[23] E.J. Gabe, P.S. White, G.D. Enright, DIFRAC: A Fortran 77 Control Routine for 4-Circle Diffractometers, NRC, Ottawa, 1995.

[24] A.C. Larson, in: F.R. Ahmed (Ed.), Crystallographic Computing, Munksgaard, Copenhagen, 1970, p. 291.

[25] E.J. Gabe, Y. LePage, J.-P. Charland, F.L. Lee, P.S. White, J. Appl. Crystallogr. 22 (1989) 384.

[26] D.J. Watkin, C.K. Prout, J.R. Carruthers, P.W. Betteridge, R.I. Cooper, CRYSTALS Issue 11.67, Chemical Crystallography Laboratory, University of Oxford, Oxford, 2001.

[27] (a) International Tables for X-ray Crystallography, Kynoch, Birmingham, UK (present distributor: Kluwer Academic Publishers, Boston, MA), 1974, Vol. IV, pp. 99.;
(b) International Tables for Crystallography, Kluwer Academic Publishers, Boston, MA, 1992, Vol. C, p. 200.

[28] R.A. Penneman, L.H. Jones, J. Inorg. Nucl. Chem. 20 (1961) 19.

[29] K.G. Ashurst, N.P. Finkelstein, L.A. Goold, J. Chem. Soc. A (1971) 1899.

[30] T. Rojo, M.I. Arriortua, J. Ruiz, J. Darriet, G. Villeneuve, D. Beltran-Porter, J. Chem. Soc., Dalton Trans. (1987) 285.

[31] M. Rodriguez, A. Llobet, M. Corbella, A.E. Martell, J. Reibenspies, Inorg. Chem. 38 (1999) 2328.

[32] A.W. Addison, T.N. Rao, J. Reedijk, J.V. Rijn, G.C. Verschoor, J. Chem. Soc., Dalton Trans. (1984) 1349.

[33] K. Brodersen, H.-U. Hummel, in: G. Wilkinson, R.D. Gillard, J.A. McCleverty (Eds.), Comprehensive Coordination Chemistry, Pergamon Press, Oxford, 1987, p. 1047.

[34] D. Grdenic, Quart. Rev. 19 (1965) 303.

[35] D.A. House, W.T. Robinson, V. McKee, Coord. Chem. Rev. 136 (1994) 533.

[36] A. Schunk, U. Thewalt, Z. Anorg. Allg. Chem. 627 (2001) 797.

[37] D.P. Graddon, Rev. Inorg. Chem. 4 (1982) 211.

[38] C.A. White, G.P.A. Yap, N.P. Raju, J.E. Greedan, R.J. Crutchley, Inorg. Chem. 38 (1999) 2548.

[39] B. Bleaney, K.D. Bowers, Proc. R. Soc. London, Ser. A 214 (1952) 451.

[40] W.E. Hatfield, W.E. Estes, W.E. Marsh, M.W. Pickens, L.W. ter Haar, R.R. Weller, in: J.S. Miller (Ed.), Extended Linear Chain Compounds, Plenum Press, New York, 1983, p. 43.

[41] H. Oshio, T. Watanabe, A. Ohto, T. Ito, U. Nagashima, Angew. Chem., Int. Ed. Engl. 33 (1994) 670.

[42] H. Oshio, T. Watanabe, A. Ohto, T. Ito, T. Ikoma, S. Tero-Kubota, Inorg. Chem. 36 (1997) 3014.

[43] L.R. Falvello, M. Tomás, Chem. Commun. (1999) 273.

[44] I. Castro, J. Faus, M. Julve, C. Bois, J.A. Real, F. Lloret, J. Chem. Soc., Dalton Trans. (1992) 47.

[45] G.D. Munno, M. Julve, F. Lloret, J. Faus, M. Verdaguer, A. Caneschi, Inorg. Chem. 34 (1995) 157.

[46] G. Grasa, F. Tuna, R. Gheorghe, D.B. Leznoff, S.J. Rettig, M. Andruh, New J. Chem. 24 (2000) 615.

[47] E. Ruiz, P. Alemany, S. Alvarez, J. Cano, J. Am. Chem. Soc. 119 (1997) 1297.

[48] E. Ruiz, P. Alemany, S. Alvarez, J. Cano, Inorg. Chem. 36 (1997) 3683.

[49] K.T. McGregor, N.T. Watkins, D.L. Lewis, R.F. Drake, D.J. Hodgson, W.E. Hatfield, Inorg. Nucl. Chem. Lett. 9 (1973) 423.

[50] V.H. Crawford, H.W. Richardson, J.R. Wasson, D.J. Hodgson, W.E. Hatfield, Inorg. Chem. 15 (1976) 2107.

[51] G.A. van Albada, I. Mutikainen, U. Turpeinen, J. Reedijk, Inorg. Chim. Acta 324 (2001) 273 (and references therein).

[52] J.J. Borrás-Almenar, E. Coronado, J. Curely, R. Georges, J.J. Gianduzzo, Inorg. Chem. 33 (1994) 5171.

[53] P. Pyykkö, Chem. Rev. 97 (1997) 597.